

CERN-TH/2001-151  
MPI-PHT-2001-16  
May 2001

# The Radiative Decays $B \rightarrow V\gamma$ at Next-to-Leading Order in QCD

STEFAN W. BOSCH <sup>a,b</sup> and GERHARD BUCHALLA <sup>a</sup>

<sup>a</sup> *Theory Division, CERN, CH-1211 Geneva 23, Switzerland*

<sup>b</sup> *Max-Planck-Institut für Physik, Werner-Heisenberg-Institut,  
Föhringer Ring 6, D-80805 Munich, Germany*

## Abstract

We provide a model-independent framework for the analysis of the radiative  $B$ -meson decays  $B \rightarrow K^*\gamma$  and  $B \rightarrow \rho\gamma$ . In particular, we give a systematic discussion of the various contributions to these exclusive processes based on the heavy-quark limit of QCD. We propose a novel factorization formula for the consistent treatment of  $B \rightarrow V\gamma$  matrix elements involving charm (or up-quark) loops, which contribute at leading power in  $\Lambda_{QCD}/m_B$  to the decay amplitude. Annihilation topologies are shown to be power suppressed. In some cases they are nevertheless calculable. The approach is similar to the framework of QCD factorization that has recently been formulated for two-body non-leptonic  $B$  decays. These results allow us, for the first time, to compute *exclusive*  $b \rightarrow s(d)\gamma$  decays systematically beyond the leading logarithmic approximation. We present results for these decays complete to next-to-leading order in QCD and to leading order in the heavy-quark limit. Phenomenological implications for various observables of interest are discussed, including direct CP violation, and isospin and U-spin breaking effects.

# 1 Introduction

The radiative transitions  $b \rightarrow s\gamma$ ,  $b \rightarrow d\gamma$  are among the most valuable probes of flavour physics. Proceeding at rates of order  $G_F^2\alpha$ , they are systematically enhanced over other loop-induced, non-radiative rare decays, which are proportional to  $G_F^2\alpha^2$ . In fact, the Cabibbo-favoured  $b \rightarrow s\gamma$  modes belong to the small number of rare decays that are experimentally accessible already at present. The inclusive branching fraction has been measured to be

$$B(B \rightarrow X_s\gamma) = (2.96 \pm 0.35) \cdot 10^{-4} \quad (1)$$

combining the results of [1, 2, 3]. The branching ratios for the exclusive channels have been determined by CLEO [4], and more recently also by BABAR [5] and BELLE [2]:

$$B(B^0 \rightarrow K^{*0}\gamma) = \begin{cases} (4.55 \pm 0.70 \pm 0.34) \cdot 10^{-5} & [4] \\ (4.39 \pm 0.41 \pm 0.27) \cdot 10^{-5} & [5] \\ (4.96 \pm 0.67 \pm 0.45) \cdot 10^{-5} & [2] \end{cases} \quad (2)$$

$$B(B^+ \rightarrow K^{*+}\gamma) = \begin{cases} (3.76 \pm 0.86 \pm 0.28) \cdot 10^{-5} & [4] \\ (3.89 \pm 0.93 \pm 0.41) \cdot 10^{-5} & [2] \end{cases} \quad (3)$$

On the theoretical side, the flavour-changing neutral current (FCNC) reactions  $b \rightarrow s(d)\gamma$  are characterized by their high sensitivity to New Physics and by the particularly large impact of short-distance QCD corrections [6, 7, 8, 9]. Considerable efforts have therefore been devoted to achieve a full calculation of the inclusive decay  $b \rightarrow s\gamma$  at next-to-leading order (NLO) in renormalization group (RG) improved perturbation theory [10, 11, 12] (see [13] for recent reviews).

Whereas the inclusive mode can be computed perturbatively, using the fact that the  $b$ -quark mass is large and employing the heavy-quark expansion, the treatment of the exclusive channel  $B \rightarrow K^*\gamma$  is in general more complicated. In this case bound state effects are essential and need to be described by nonperturbative hadronic quantities (form factors). The basic mechanisms at next-to-leading order were already discussed previously for the  $B \rightarrow V\gamma$  amplitudes [14]. However, hadronic models were used to evaluate the various contributions, which did not allow a clear separation of short- and long-distance dynamics and a clean distinction of model-dependent and model-independent features.

In this paper we present a systematic analysis of the exclusive radiative decays  $B \rightarrow V\gamma$  ( $V = K^*, \rho$ ) in QCD, based on the heavy quark limit  $m_b \gg \Lambda_{QCD}$ . We shall establish factorization formulas for the evaluation of the relevant hadronic matrix elements of local operators in the weak Hamiltonian. Factorization holds in QCD to leading power in the heavy quark limit. This result relies on arguments similar to those used previously to demonstrate QCD factorization for hadronic two-body modes of the type  $B \rightarrow \pi\pi$  [15, 16].

This framework will allow us to separate perturbatively calculable contributions from the nonperturbative form factors and universal meson light-cone distribution amplitudes (LCDA) in a systematic way. This includes the treatment of

loop effects from light quarks, in particular up and charm. Such loop effects are straightforwardly included for the inclusive decays  $b \rightarrow s(d)\gamma$ . For the exclusive modes, however, the effects from virtual charm and up quarks have so far been considered to be uncalculable “long-distance” contributions and have never been treated in a model independent fashion.

Finally, power counting in  $\Lambda_{QCD}/m_b$  implies a hierarchy among the possible mechanisms for  $B \rightarrow V\gamma$  transitions. This allows us to identify leading and subleading contributions. For example, weak annihilation contributes only at subleading power in the heavy quark limit.

Within this approach, higher order QCD corrections can be consistently taken into account. We give the  $B \rightarrow V\gamma$  decay amplitudes at next-to-leading order (NLO). After including NLO corrections the largest uncertainties still come from the  $B \rightarrow V$  form factors, which are at present known only with limited precision ( $\sim \pm 15\%$ ), mostly from QCD sum rule calculations [17]. The situation should improve in the future with the help of both lattice QCD [18] and analytical methods based on the heavy-quark and large-energy limits [19, 20, 21].

Despite the more complicated theoretical situation of the exclusive channels in comparison to the inclusive decays, the goal of obtaining a better understanding of the exclusive modes is very well motivated. This is because the exclusive decays are easier to investigate experimentally, especially in the difficult environment of hadron machines as the Fermilab Tevatron or the LHC at CERN. In any case the systematic uncertainties, both experimental and theoretical, are very different for  $B \rightarrow V\gamma$  and  $b \rightarrow s(d)\gamma$ . A careful study of the exclusive modes can therefore yield valuable complementary information in testing the Standard Model.

The remainder of this paper is organized as follows. In section 2 we collect basic expressions and present the structure of the QCD factorization formulas for  $B \rightarrow V\gamma$  matrix elements in general terms. Sections 3 and 4 give a detailed discussion of  $B \rightarrow K^*\gamma$  and  $B \rightarrow \rho\gamma$ , respectively. Phenomenological applications are studied in section 5. Finally, section 6 contains our conclusions.

## 2 Basic Formulas

The effective Hamiltonian for  $b \rightarrow s\gamma$  transitions reads

$$\mathcal{H}_{eff} = \frac{G_F}{\sqrt{2}} \sum_{p=u,c} \lambda_p^{(s)} \left[ C_1 Q_1^p + C_2 Q_2^p + \sum_{i=3,\dots,8} C_i Q_i \right] \quad (4)$$

where

$$\lambda_p^{(s)} = V_{ps}^* V_{pb} \quad (5)$$

The operators are given by

$$Q_1^p = (\bar{s}p)_{V-A} (\bar{p}b)_{V-A} \quad (6)$$

$$Q_2^p = (\bar{s}_i p_j)_{V-A} (\bar{p}_j b_i)_{V-A} \quad (7)$$

$$Q_3 = (\bar{s}b)_{V-A} \sum_q (\bar{q}q)_{V-A} \quad (8)$$

$$Q_4 = (\bar{s}_i b_j)_{V-A} \sum_q (\bar{q}_j q_i)_{V-A} \quad (9)$$

$$Q_5 = (\bar{s}b)_{V-A} \sum_q (\bar{q}q)_{V+A} \quad (10)$$

$$Q_6 = (\bar{s}_i b_j)_{V-A} \sum_q (\bar{q}_j q_i)_{V+A} \quad (11)$$

$$Q_7 = \frac{e}{8\pi^2} m_b \bar{s}_i \sigma^{\mu\nu} (1 + \gamma_5) b_i F_{\mu\nu} \quad (12)$$

$$Q_8 = \frac{g}{8\pi^2} m_b \bar{s}_i \sigma^{\mu\nu} (1 + \gamma_5) T_{ij}^a b_j G_{\mu\nu}^a \quad (13)$$

The most important operators are  $Q_{1,2}^p$  and the magnetic penguin operator  $Q_7$ . Note that in our notation the numbering of  $Q_{1,2}^p$  is reversed with respect to the convention of [22], i.e.  $C_1^{(0)}(M_W) = 1$  and  $C_2^{(0)}(M_W) = 0$ . The sign conventions for the electromagnetic and strong couplings correspond to the covariant derivative  $D_\mu = \partial_\mu + ieQ_f A_\mu + igT^a A_\mu^a$ . With these definitions the coefficients  $C_{7,8}$  are negative in the Standard Model, which is the choice generally adopted in the literature. The effective Hamiltonian for  $b \rightarrow d\gamma$  is obtained from (4–13) by the replacement  $s \rightarrow d$ . The Wilson coefficients  $C_i$  in (4) are known at next-to-leading order [12].

The most difficult step in computing the decay amplitudes is the evaluation of the hadronic matrix elements of the operators in (4). A systematic treatment can be given in the heavy-quark limit. We will argue that in this case the following factorization formula is valid

$$\langle V\gamma(\epsilon)|Q_i|\bar{B}\rangle = \left[ F^{B \rightarrow V}(0) T_i^I + \int_0^1 d\xi dv T_i^{II}(\xi, v) \Phi_B(\xi) \Phi_V(v) \right] \cdot \epsilon \quad (14)$$

where  $\epsilon$  is the photon polarization 4-vector. Here  $F^{B \rightarrow V}$  is a  $B \rightarrow V$  transition form factor, and  $\Phi_B$ ,  $\Phi_V$  are leading twist light-cone distribution amplitudes of the  $B$  meson and the vector meson  $V$ , respectively. These quantities are universal, nonperturbative objects. They describe the long-distance dynamics of the matrix elements, which is factorized from the perturbative, short-distance interactions expressed in the hard-scattering kernels  $T_i^I$  and  $T_i^{II}$ . The QCD factorization formula (14) holds up to corrections of relative order  $\Lambda_{QCD}/m_b$ .

For  $Q_7$  the factorization formula (14) is trivial. The matrix element is simply expressed in terms of the standard form factor,  $T_7^I$  is a purely kinematical function and the spectator term  $T_7^{II}$  is absent. An illustration is given in Fig. 1. The matrix element reads

$$\langle V(k, \eta) \gamma(q, \epsilon) | Q_7 | \bar{B} \rangle = -\frac{e}{2\pi^2} m_b c_V F_V \left[ \varepsilon^{\mu\nu\lambda\rho} \epsilon_\mu \eta_\nu k_\lambda q_\rho + i(\epsilon \cdot \eta k \cdot q - \epsilon \cdot k \eta \cdot q) \right] \quad (15)$$

where  $c_V = 1$  for  $V = K^*$ ,  $\rho^-$  and  $c_V = 1/\sqrt{2}$  for  $V = \rho^0$ . The  $\bar{B} \rightarrow V$  form factor  $F_V$  is evaluated at momentum transfer  $q^2 = 0$ . Our phase conventions

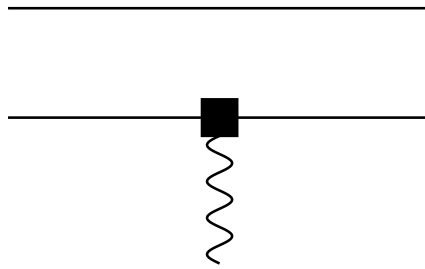


Figure 1: Contribution of the magnetic penguin operator  $Q_7$  described by  $B \rightarrow V$  form factors. All possible gluon exchanges between the quark lines are included in the form factors and have not been drawn explicitly.

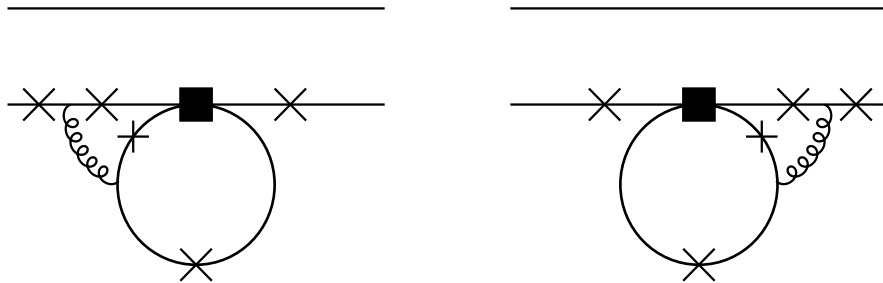


Figure 2:  $\mathcal{O}(\alpha_s)$  contribution to the hard-scattering kernels  $T_i^I$  from four-quark operators  $Q_i$ . The crosses indicate the places where the emitted photon can be attached.

coincide with those of [17, 23]. In particular we have  $F_V > 0$ ,  $\varepsilon^{0123} = -1$ , and the phases of  $V$  (with flavour content  $\bar{q}q'$ ) and  $\bar{B}$  are such that

$$\langle V(k, \eta) | \bar{q} \sigma_{\mu\nu} q' | 0 \rangle = -i(\eta_\mu k_\nu - \eta_\nu k_\mu) f_V^\perp \quad (16)$$

$$\langle 0 | \bar{u} \gamma_\mu \gamma_5 b | \bar{B}(p) \rangle = +i f_B p_\mu \quad (17)$$

with positive  $f_B$ ,  $f_V^\perp$ . In the leading logarithmic approximation (LO) and to leading power in the heavy-quark limit,  $Q_7$  gives the only contribution to the amplitude of  $\bar{B} \rightarrow V\gamma$ .

The matrix elements of the four-quark operators  $Q_i$  (and of  $Q_8$ ) start contributing at  $\mathcal{O}(\alpha_s)$ . In this case the factorization formula becomes nontrivial. The diagrams for the hard-scattering kernels  $T_i^I$  are shown in Fig. 2 for  $Q_1, \dots, Q_6$  and in Fig. 3 for  $Q_8$ . The non-vanishing contributions to  $T_i^{II}$  are shown in Fig. 4.

The diagrams in Figs. 2 – 4 represent the complete set of contributions from  $Q_{1,2}$  and  $Q_8$  to leading order in the heavy-quark limit and at  $\mathcal{O}(\alpha_s)$ . The first term in the factorization formula (14) is given by the form factor from (15) and the hard-scattering kernels  $T_i^I$ . The latter are calculable functions of  $m_q/m_b$ , where  $m_q$  is the mass of the internal quarks in the loop diagram. For the second term in (14), where the spectator quark is involved, we need light-cone distribution

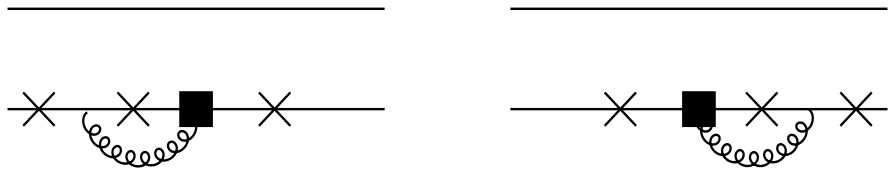


Figure 3:  $\mathcal{O}(\alpha_s)$  contribution to the hard-scattering kernels  $T_8^I$  from chromomagnetic penguin operator  $Q_8$ .

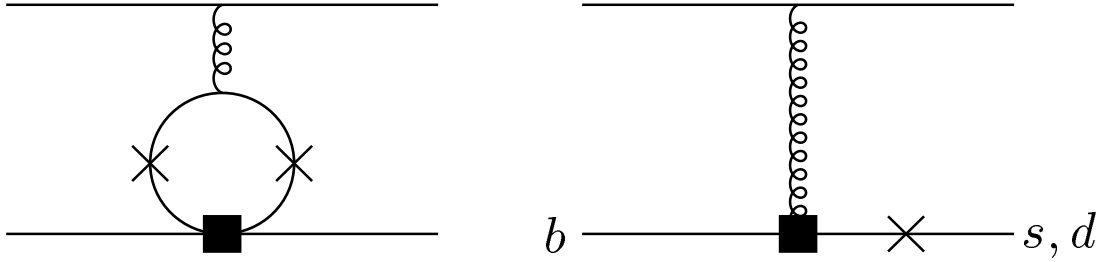


Figure 4:  $\mathcal{O}(\alpha_s)$  contribution to the hard-scattering kernels  $T_i^{II}$  from four-quark operators  $Q_i$  (left) and from  $Q_8$ .

amplitudes (wave functions) for  $B$  mesons and light vector mesons. In the case of the  $B$  meson we have to leading power [16, 20]

$$\langle 0 | b(0) \bar{u}(z) | \bar{B}(p) \rangle = \frac{if_B}{4} (\not{p} + m_b) \gamma_5 \int_0^1 d\xi e^{-i\xi p^+ z^-} [\Phi_{B1}(\xi) + \not{\xi} \Phi_{B2}(\xi)] \quad (18)$$

with  $n = (1, 0, 0, -1)$ , chosen to be parallel to the 4-momentum of the vector meson. The functions  $\Phi_{1,2}(\xi)$  describe the distribution of light-cone momentum fraction  $\xi = l_+/p_+$  of the spectator quark with momentum  $l$  inside the  $B$  meson. Here light-cone components of four-vectors  $v$  are defined by

$$v_\pm = \frac{v^0 \pm v^3}{\sqrt{2}} \quad (19)$$

The wave functions are highly asymmetric with  $\xi = \mathcal{O}(\Lambda_{QCD}/m_b)$ . They are normalized as

$$\int_0^1 d\xi \Phi_{B1}(\xi) = 1 \quad \int_0^1 d\xi \Phi_{B2}(\xi) = 0 \quad (20)$$

The first negative moment of  $\Phi_{B1}(\xi)$ , which will be needed below, can be parametrized by a quantity  $\lambda_B = \mathcal{O}(\Lambda_{QCD})$ , i.e.

$$\int_0^1 d\xi \frac{\Phi_{B1}(\xi)}{\xi} = \frac{m_B}{\lambda_B} \quad (21)$$

In  $\bar{B} \rightarrow V\gamma$  decays the vector meson is transversely polarized. The leading-twist and leading-power distribution amplitude for light vector mesons with trans-

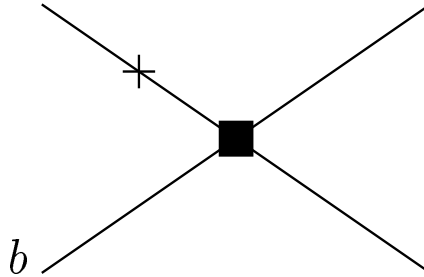


Figure 5: Annihilation contribution to  $\bar{B} \rightarrow V\gamma$  decay. The dominant mechanism is the radiation of the photon from the light quark in the  $B$  meson, as shown. This amplitude is suppressed by one power of  $\Lambda_{QCD}/m_b$ , but it is still calculable in QCD factorization. Radiation of the photon from the remaining three quark lines is suppressed by  $(\Lambda_{QCD}/m_b)^2$  for operators  $Q_{1,2}$ .

verse polarization,  $\Phi_\perp$ , is defined by

$$\langle V(k, \eta) | \bar{q}'(z) \bar{q}(0) | 0 \rangle = \frac{if_V^\perp}{4} \sigma^{\mu\nu} \eta_\mu k_\nu \int_0^1 dv e^{i\bar{v}k \cdot z} \Phi_\perp(v) \quad (22)$$

Here and in the following we use the short-hand notation

$$\bar{v} \equiv 1 - v \quad (23)$$

for light-cone variables.

The light-cone wave function  $\Phi_\perp$  has an expansion in terms of Gegenbauer polynomials  $C_n^{3/2}(2v - 1)$

$$\Phi_\perp(v) = 6v(1 - v) \left[ 1 + \sum_{n=1}^{\infty} \alpha_n^\perp(\mu) C_n^{3/2}(2v - 1) \right] \quad (24)$$

where  $C_1^{3/2}(x) = 3x$ ,  $C_2^{3/2}(x) = \frac{3}{2}(5x^2 - 1)$ , etc. The Gegenbauer moments  $\alpha_n^\perp(\mu)$  are multiplicatively renormalized. They vanish logarithmically as the scale  $\mu \rightarrow \infty$ . In this limit  $\Phi_\perp$  reduces to its asymptotic form  $\Phi_\perp(v) = 6v\bar{v}$ , which often is a reasonable first approximation. The remaining leading-twist light-cone wave functions for light vector mesons,  $\Phi_\parallel$ ,  $g_\perp^{(v)}$  and  $g_\perp^{(a)}$  [17, 24], do not contribute at leading power if the mesons are transversely polarized.

The form factor  $F_V$ ,  $f_B/\lambda_B$ , and the light-cone wave function  $f_V^\perp \Phi_\perp(v)$  are the nonperturbative quantities required to describe  $\bar{B} \rightarrow V\gamma$  at next-to-leading order in QCD. ( $\Phi_{B2}(\xi)$  does not contribute.)

There are further mechanisms that can in principle contribute to  $\bar{B} \rightarrow V\gamma$  decays. One possibility is weak annihilation, depicted in Fig. 5. In this case the leading-power projection onto the meson  $V$  in (22) vanishes, because the trace over an odd number of Dirac matrices is zero. A non-vanishing result arises from the projector

$$\langle V(k, \eta) | \bar{q} \gamma_\nu q' | 0 \rangle = f_V m_V \eta_\nu \quad (25)$$

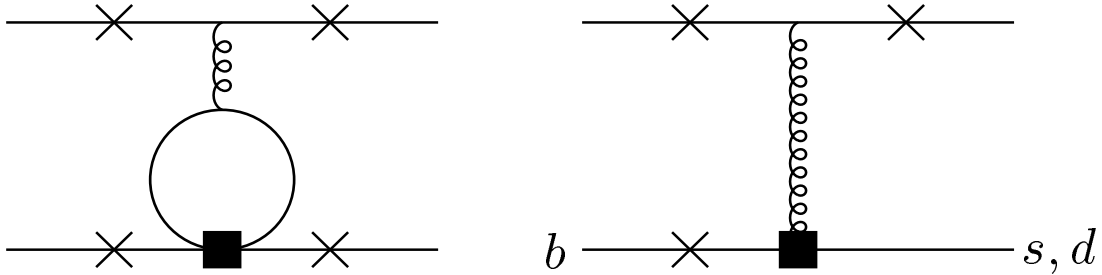


Figure 6: Other contributions that are power-suppressed in the heavy-quark limit.

which, however, is suppressed by one power of  $\Lambda_{QCD}/m_b$  compared to (16), (22) for transverse polarization  $\eta_\nu$  ( $f_V, f_V^\perp, m_V \sim \Lambda_{QCD}, k \sim m_b$ ). This results in a corresponding power suppression of weak annihilation. The dominant contribution comes from the diagram shown in Fig. 5. Here the photon is emitted from the light-quark constituent in the  $B$  meson, which leads to a quark propagator scaling as  $1/\Lambda_{QCD}$ . This is in contrast to the remaining three possible diagrams with a quark propagator  $\sim 1/m_b$ . The latter contributions are therefore even stronger suppressed,  $\sim (\Lambda_{QCD}/m_b)^2$  relative to the leading  $\bar{B} \rightarrow V\gamma$  amplitude.

Despite its power suppression, the dominant annihilation amplitude can be computed within QCD factorization. This is because the colour-transparency argument applies to the emitted, highly energetic vector meson in the heavy-quark limit [16]. A similar observation was already made in [25]. On the other hand, we disagree with the claim made in this paper that the  $\mathcal{O}(\alpha_s)$  correction to Fig. 5 would vanish identically in the chiral limit and to leading-twist order. This claim is based on the observation that the projector in (22) gives zero when applied to a current with an odd number of Dirac matrices. However, by the same argument, the diagram in Fig. 5 would vanish even at leading order in  $\alpha_s$ , which is not the case. The proper treatment of the  $\mathcal{O}(\alpha_s)$  correction should employ the subleading-power projections related to the wave functions  $\Phi_{\parallel}, g_{\perp}^{(v)}, g_{\perp}^{(a)}$  [17, 24], corresponding to the use of (25) at  $\mathcal{O}(\alpha_s^0)$ . This correction has not yet been computed, but we see no a-priori reason to expect a vanishing result.

Since weak annihilation is a power correction, we will content ourselves with the lowest order result ( $\mathcal{O}(\alpha_s^0)$ ) for our estimates below. In particular, we shall include the annihilation effects from operators  $Q_{1,2}$  to estimate isospin-breaking corrections in  $B \rightarrow \rho\gamma$  decays. The reason for including this class of power corrections is that they come with a numerical enhancement from the large Wilson coefficients  $C_{1,2}$  ( $C_1 \approx 3|C_7|$ ) and are not CKM suppressed. Instead, a CKM suppression of annihilation effects occurs for  $B \rightarrow K^*\gamma$  and these contributions are thus very small in this case.

Finally, Fig. 6 displays the remaining diagrams with a power suppression. The penguin-annihilation diagrams (left) are power suppressed in a way similar to the ordinary annihilation topologies. The spectator diagrams from  $Q_8$  (right)

lead to amplitudes that are either manifestly power-suppressed (photon emitted from the quark line in the upper right), or that are superficially of leading power, but vanish when the leading-order projections are performed (photon emitted from either of the quarks forming the  $B$  meson). Recall, however, that photon emission from the light-quark line from  $Q_8$  is a leading-power effect (see Fig. 4).

### 3 $B \rightarrow K^* \gamma$

In the case of  $B \rightarrow K^* \gamma$  the component of the Hamiltonian (4) proportional to  $\lambda_u$  is strongly CKM suppressed ( $|\lambda_u/\lambda_c| \approx 0.02$ ) and has only a minor impact on the decay rate. It is essentially negligible, but will be included later on for completeness. Throughout this work we shall neglect the contribution from the QCD penguin operators  $Q_3, \dots, Q_6$ , which enter at  $\mathcal{O}(\alpha_s)$  and are further suppressed by very small Wilson coefficients. We note that to  $\mathcal{O}(\alpha_s)$  the matrix element of  $Q_2$  is zero because of its colour structure. The amplitude for  $\bar{B} \rightarrow K^* \gamma$  then reads ( $\langle Q_i \rangle \equiv \langle K^* \gamma | Q_i | \bar{B} \rangle$ )

$$A(\bar{B} \rightarrow K^* \gamma) = \frac{G_F}{\sqrt{2}} \lambda_c^{(s)} (C_7 \langle Q_7 \rangle + C_1 \langle Q_1^c \rangle + C_8 \langle Q_8 \rangle) \quad (26)$$

The leading-order matrix element  $\langle Q_7 \rangle$  is given in (15) with  $V \equiv K^*$ . At sub-leading order in  $\alpha_s$  the matrix elements  $\langle Q_{1,8} \rangle$  need to be computed from the diagrams in Figs. 2 – 4. The result for the diagrams in Figs. 2 and 3, which enter the hard-scattering kernels  $T_1^I, T_8^I$ , can be inferred from [11]. In these papers the diagrams were computed to obtain the matrix elements for the inclusive mode  $b \rightarrow s\gamma$  at next-to-leading order. In this context Figs. 2 and 3 represented the virtual corrections to the inclusive matrix elements of  $Q_1$  and  $Q_8$ . In our case they determine the kernels  $T_1^I$  and  $T_8^I$ . As required for the consistency of the factorization formula these corrections must be dominated by hard scales  $\sim m_b$  and hence must be infrared finite. This is indeed the case. Re-interpreted as the perturbative hard-scattering kernels for the exclusive process, the results from [11] imply

$$\langle Q_{1,8} \rangle^I = \langle Q_7 \rangle \frac{\alpha_s C_F}{4\pi} G_{1,8} \quad (27)$$

where  $C_F = (N^2 - 1)/(2N)$ , with  $N = 3$  the number of colours, and

$$G_1(s_c) = -\frac{104}{27} \ln \frac{\mu}{m_b} + g_1(s_c) \quad (28)$$

$$G_8 = \frac{8}{3} \ln \frac{\mu}{m_b} + g_8 \quad (29)$$

$$\begin{aligned} g_1(s) = & -\frac{833}{162} - \frac{20i\pi}{27} + \frac{8\pi^2}{9} s^{3/2} \\ & + \frac{2}{9} \left[ 48 + 30i\pi - 5\pi^2 - 2i\pi^3 - 36\zeta(3) + (36 + 6i\pi - 9\pi^2) \ln s \right. \end{aligned}$$

$$\begin{aligned}
& + (3 + 6i\pi) \ln^2 s + \ln^3 s \Big] s \\
& + \frac{2}{9} \left[ 18 + 2\pi^2 - 2i\pi^3 + (12 - 6\pi^2) \ln s + 6i\pi \ln^2 s + \ln^3 s \right] s^2 \\
& + \frac{1}{27} \left[ -9 + 112i\pi - 14\pi^2 + (182 - 48i\pi) \ln s - 126 \ln^2 s \right] s^3 \quad (30)
\end{aligned}$$

$$g_8 = \frac{11}{3} - \frac{2\pi^2}{9} + \frac{2i\pi}{3} \quad (31)$$

Here we denote

$$s_c = \frac{m_c^2}{m_b^2} \quad (32)$$

We now turn to the mechanism where the spectator participates in the hard scattering.

To find the correction for  $\langle Q_1 \rangle$  we compute the first diagram in Fig. 4, using the light-cone projectors in (18) and (22). We obtain

$$\langle Q_1 \rangle^{II} = \langle Q_7 \rangle \frac{\alpha_s(\mu_h) C_F}{4\pi} H_1(s_c) \quad (33)$$

with

$$H_1(s) = -\frac{2\pi^2}{3N} \frac{f_B f_V^\perp}{F_V m_B^2} \int_0^1 d\xi \frac{\Phi_{B1}(\xi)}{\xi} \int_0^1 dv h(\bar{v}, s) \Phi_\perp(v) \quad (34)$$

The hard-scattering function  $h(u, s)$  is given by

$$h(u, s) = \frac{4s}{u^2} \left[ L_2 \left( \frac{2}{1 - \sqrt{\frac{u-4s+i\varepsilon}{u}}} \right) + L_2 \left( \frac{2}{1 + \sqrt{\frac{u-4s+i\varepsilon}{u}}} \right) \right] - \frac{2}{u} \quad (35)$$

$L_2$  is the dilogarithmic function

$$L_2(x) = - \int_0^x dt \frac{\ln(1-t)}{t} \quad (36)$$

The function  $h(u, s)$  is real for  $u \leq 4s$  and develops an imaginary part for  $u > 4s$ . At small values of  $u$  it has the expansion

$$h(u, s) = \frac{1}{6s} + \frac{1}{45s^2} u + \mathcal{O} \left( \frac{u^2}{s^3} \right) \quad (37)$$

It is also regular for  $s \rightarrow 0$

$$h(u, 0) = -\frac{2}{u} \quad (38)$$

The function  $h(\bar{v}, s_c)$  is displayed in Fig. 7.

The correction to  $\langle Q_8 \rangle$  from the hard spectator interaction comes from the second diagram in Fig. 4. One finds

$$\langle Q_8 \rangle^{II} = \langle Q_7 \rangle \frac{\alpha_s(\mu_h) C_F}{4\pi} H_8 \quad (39)$$

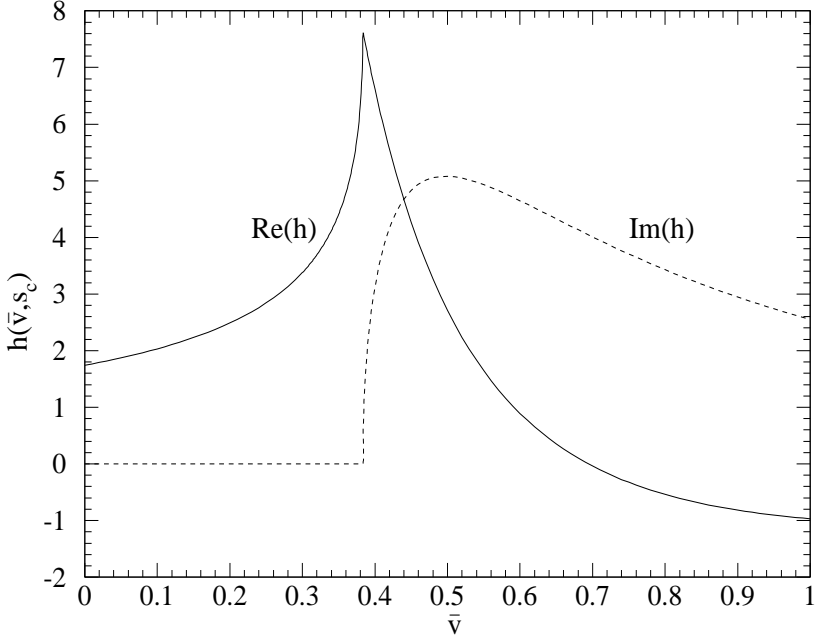


Figure 7: The hard-scattering kernel  $h(\bar{v}, s_c)$  as a function of  $\bar{v}$ .

where

$$H_8 = \frac{4\pi^2}{3N} \frac{f_B f_V^\perp}{F_V m_B^2} \int_0^1 d\xi \frac{\Phi_{B1}(\xi)}{\xi} \int_0^1 dv \frac{\Phi_\perp(v)}{v} \quad (40)$$

The gluons in Fig. 4 transfer a momentum of order  $\mu_h \sim \sqrt{\Lambda_{QCD} m_b}$ . Therefore we set  $\alpha_s = \alpha_s(\mu_h)$  in (33) and (39). For our numerical analysis we shall use  $\mu_h = \sqrt{\Lambda_h \mu}$  with  $\Lambda_h = 0.5$  GeV and  $\mu = \mathcal{O}(m_b)$ .

Finally, we can combine these results and write, including also the up-quark contribution,

$$A(\bar{B} \rightarrow K^* \gamma) = \frac{G_F}{\sqrt{2}} \left[ \sum_p \lambda_p^{(s)} a_7^p(K^* \gamma) \right] \langle K^* \gamma | Q_7 | \bar{B} \rangle \quad (41)$$

where, at NLO

$$\begin{aligned} a_7^p(V\gamma) = & C_7 + \frac{\alpha_s(\mu) C_F}{4\pi} (C_1(\mu) G_1(s_p) + C_8(\mu) G_8) \\ & + \frac{\alpha_s(\mu_h) C_F}{4\pi} (C_1(\mu_h) H_1(s_p) + C_8(\mu_h) H_8) \end{aligned} \quad (42)$$

Here the NLO expression for  $C_7$  has to be used, while the leading order values are sufficient for  $C_1$  and  $C_8$ . The explicit formulas for the Wilson coefficients can be found in [12].

The scale dependence of the matrix element of  $Q_7$  is reflected in the running of the product of  $b$ -quark mass and form factor which is explicitly given as

$$(m_b \cdot F_V)[\mu] = (m_b \cdot F_V)[m_b] \left( 1 - \frac{\alpha_s(\mu)}{4\pi} 8C_F \ln \frac{\mu}{m_b} \right) \quad (43)$$

This dependence on the scale  $\mu$  has to be taken into account when the residual scale dependence of physical quantities is investigated.

From the amplitude in (41) the branching ratio is obtained as

$$B(\bar{B} \rightarrow K^* \gamma) = \tau_B \frac{G_F^2 \alpha m_B^3 m_b^2}{32\pi^4} \left( 1 - \frac{m_{K^*}^2}{m_B^2} \right)^3 \left| \sum_p \lambda_p^{(s)} a_7^p(K^* \gamma) \right|^2 |F_{K^*}|^2 \quad (44)$$

## 4 $B \rightarrow \rho\gamma$

For the decay  $\bar{B} \rightarrow \rho\gamma$  both sectors of the effective Hamiltonian have the same order of magnitude and have to be included. It is straightforward to translate the expressions from the previous section to this case. The amplitude can be written as

$$A(\bar{B} \rightarrow \rho\gamma) = \frac{G_F}{\sqrt{2}} \left[ \sum_p \lambda_p^{(d)} a_7^p(\rho\gamma) \right] \langle \rho\gamma | Q_7 | \bar{B} \rangle \quad (45)$$

where  $a_7^p(V\gamma)$  is given in (42). The branching fraction becomes

$$B(\bar{B} \rightarrow \rho\gamma) = \tau_B \frac{G_F^2 \alpha m_B^3 m_b^2}{32\pi^4} \left( 1 - \frac{m_\rho^2}{m_B^2} \right)^3 \left| \sum_p \lambda_p^{(d)} a_7^p(\rho\gamma) \right|^2 c_\rho^2 |F_\rho|^2 \quad (46)$$

The rate for the CP-conjugated mode  $B \rightarrow \rho\gamma$  is obtained by replacing  $\lambda_p^{(d)} \rightarrow \lambda_p^{(d)*}$ . We may then consider the CP asymmetry

$$\mathcal{A}_{CP}(\rho\gamma) = \frac{\Gamma(B \rightarrow \rho\gamma) - \Gamma(\bar{B} \rightarrow \rho\gamma)}{\Gamma(B \rightarrow \rho\gamma) + \Gamma(\bar{B} \rightarrow \rho\gamma)} \quad (47)$$

A non-vanishing CP asymmetry appears at  $\mathcal{O}(\alpha_s)$  only. Expanding  $\mathcal{A}_{CP}$  in  $\alpha_s$  and using the improved Wolfenstein parametrization for the CKM elements we obtain

$$\begin{aligned} \mathcal{A}_{CP}(\rho\gamma) &= \frac{2 \operatorname{Im} \lambda_u^{(d)*} \lambda_c^{(d)}}{|\lambda_t^{(d)}|^2} \frac{\operatorname{Im} a_7^{u*} a_7^c}{|C_7|^2} \\ &= -\frac{2\bar{\eta}}{(1-\bar{\rho})^2 + \bar{\eta}^2} \frac{\alpha_s C_F}{4\pi} \frac{C_1}{C_7} \operatorname{Im} (G_1(s_c) + H_1(s_c) - G_1(0) - H_1(0)) \end{aligned} \quad (48)$$

As we have discussed above, weak annihilation from the leading operators  $Q_{1,2}$  contributes to the  $\bar{B} \rightarrow \rho\gamma$  amplitude only at  $\mathcal{O}(\Lambda_{QCD}/m_b)$ , but is enhanced by large Wilson coefficients. These effects can be calculated in QCD factorization.

To lowest order in  $\alpha_s$  we obtain from the diagram in Fig. 5, using the projection in (25)

$$A_{ann}(B^- \rightarrow \rho^-\gamma) = \frac{G_F}{\sqrt{2}} \lambda_u^{(d)} a_1 b_u \langle \rho^-\gamma | Q_7 | B^- \rangle \quad (49)$$

$$A_{ann}(\bar{B}^0 \rightarrow \rho^0\gamma) = \frac{G_F}{\sqrt{2}} \lambda_u^{(d)} a_2 b_d \langle \rho^0\gamma | Q_7 | \bar{B}^0 \rangle \quad (50)$$

Here

$$a_{1,2} = C_{1,2} + \frac{1}{N} C_{2,1} \quad (51)$$

(evaluated in leading logarithmic approximation) and

$$b_u = \frac{2\pi^2 Q_u f_B f_\rho m_\rho}{F_\rho m_B^2 \lambda_B} \quad b_d = \frac{1}{2} b_u \quad (52)$$

Recalling that  $F_\rho \sim m_b^{-3/2}$ ,  $f_B \sim m_b^{-1/2}$  in the heavy-quark limit, we note that  $b_u \sim \Lambda_{QCD}/m_b$ . This shows explicitly the power suppression of weak annihilation. The ratio of  $b_d$  to  $b_u$  is  $-Q_d/Q_u = 1/2$ , where the minus sign comes from the relative sign between the up-quark and down-quark components of the  $\rho^0$  wave function (only the up-quarks produce the  $\rho^0$  in the annihilation process, while only the down-quarks are relevant in  $\langle Q_7 \rangle$ ).

The annihilation components are included in the decay amplitudes by substituting

$$a_7^u \rightarrow a_7^u + b_u a_1 \quad \text{for} \quad B^- \rightarrow \rho^-\gamma \quad (53)$$

$$a_7^u \rightarrow a_7^u + b_d a_2 \quad \text{for} \quad \bar{B}^0 \rightarrow \rho^0\gamma \quad (54)$$

The annihilation contribution for  $B^- \rightarrow K^{*-}\gamma$  is similar to the one for  $B^- \rightarrow \rho^-\gamma$ , with obvious replacements  $\rho \rightarrow K^*$  in  $b_u$ . Its impact is very small for  $B^- \rightarrow K^{*-}\gamma$  because of the strong CKM suppression of the up-quark sector. It will be included in our numerical analysis for definiteness. Within our approximations weak annihilation gives no contribution to  $\bar{B}^0 \rightarrow \bar{K}^{*0}\gamma$ .

## 5 Phenomenology

In this section we present numerical results for various observables of interest for the phenomenology of  $B \rightarrow V\gamma$  decays, based on the NLO QCD expressions derived in this paper. Our choice of input parameters is summarized in Table 1. Our default choice for the CKM angle  $\gamma$  is 58 deg.

We begin with the numerical result for the NLO QCD coefficient  $a_7^c(K^*\gamma)$  as a typical example. For central values of all parameters, at  $\mu = m_b$ , and displaying separately the size of the various correction terms, we find

$$\begin{aligned} a_7^c(K^*\gamma) &= -0.3221 \quad +0.0113 \quad -0.0820 - 0.0147i \quad -0.0144 - 0.0109i \\ &\quad C_7^{LO} \quad \Delta C_7^{NLO} \quad T_{1,8}^I\text{-contribution} \quad T_{1,8}^{II}\text{-contribution} \\ &= -0.4072 - 0.0256i. \end{aligned} \quad (55)$$

Table 1: Summary of input parameters.

CKM parameters and coupling constants					
$V_{us}$	$V_{cb}$	$ V_{ub}/V_{cb} $	$\Lambda_{\overline{MS}}^{(5)}$	$\alpha$	$G_F$
0.22	0.041	$0.085 \pm 0.025$	225 MeV	1/137	$1.166 \times 10^{-5} \text{ GeV}^{-2}$
Parameters related to the $B$ mesons					
$m_B$	$f_B$	$\lambda_B$		$\tau_{B^+}$	$\tau_{B^0}$
5.28 GeV	180 MeV	$(350 \pm 150)$ MeV		1.65 ps	1.56 ps
Parameters related to the $K^*$ meson [17]					
$F_{K^*}$	$f_{K^*}^\perp$	$m_{K^*}$	$\alpha_1^{K^*}$	$\alpha_2^{K^*}$	$f_{K^*}$
$0.38 \pm 0.06$	185 MeV	894 MeV	0.2	0.04	230 MeV
Parameters related to the $\rho$ meson [17]					
$F_\rho$	$f_\rho^\perp$	$m_\rho$	$\alpha_1^\rho$	$\alpha_2^\rho$	$f_\rho$
$0.29 \pm 0.04$	160 MeV	770 MeV	0	0.2	200 MeV
Quark and W-boson masses					
$m_b(m_b)$	$m_c(m_b)$	$m_{t,\text{pole}}$	$M_W$		
4.2 GeV	$(1.3 \pm 0.2)$ GeV	174 GeV	80.4 GeV		

Table 2: Predictions for branching ratios and CP asymmetries with the errors from the individual input uncertainties.

	$B(\bar{B}^0 \rightarrow \bar{K}^{*0}\gamma)[10^{-5}]$	$B(B^- \rightarrow \rho^-\gamma)[10^{-6}]$	$\mathcal{A}_{CP}(\rho^\pm\gamma)[\%]$
central	7.09	1.58	9.89
$F_{K^*}$	$+2.32/-1.99$	—	—
$F_\rho$	—	$+0.42/-0.37$	$+0.12/-0.13$
$\mu$	$+0.67/-1.00$	$+0.07/-0.19$	$+5.25/-2.40$
$\lambda_B$	$+0.38/-0.15$	$+0.26/-0.09$	$+0.35/-0.28$
$m_c$	$+0.38/-0.43$	$+0.12/-0.12$	$+1.40/-1.52$
$ V_{ub}/V_{cb} $	$+0.05/-0.05$	$+0.15/-0.13$	$+3.48/-3.30$

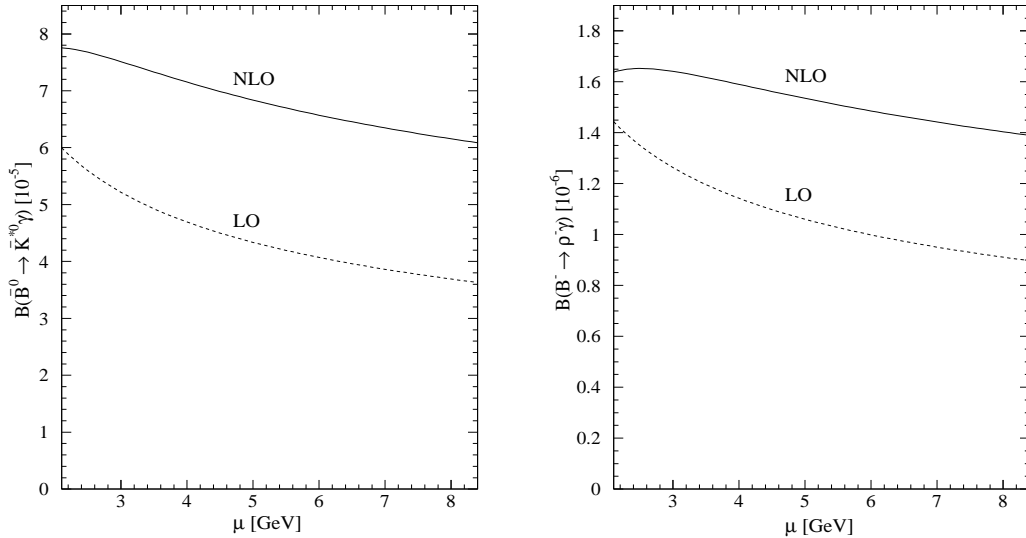


Figure 8: Dependence of the branching fractions  $B(\bar{B}^0 \rightarrow \bar{K}^{*0}\gamma)$  and  $B(B^- \rightarrow \rho^-\gamma)$  on the renormalization scale  $\mu$  at leading and next-to-leading order.

We note a sizable enhancement of the leading order value, dominated by the  $T^I$ -type correction. This feature was already observed in the context of the inclusive case in [11]. A complex phase is generated at NLO, where the  $T^I$ -corrections and the hard-spectator interactions ( $T^{II}$ ) yield comparable effects.

The net enhancement of  $a_7$  at NLO leads to a corresponding enhancement of the branching ratios, for fixed value of the form factor. This is illustrated in Fig. 8, where we show the residual scale dependence for  $B(\bar{B} \rightarrow \bar{K}^{*0}\gamma)$  and  $B(B^- \rightarrow \rho^-\gamma)$  at leading and next-to-leading order.

The sensitivity of the  $\bar{B} \rightarrow \bar{K}^{*0}\gamma$  and  $B^- \rightarrow \rho^-\gamma$  branching ratios, and of the CP asymmetry  $\mathcal{A}_{CP}(\rho\gamma)$  to variations in the relevant input parameters are summarized in Table 2. The uncertainty of the branching fractions is currently dominated by the form factors  $F_{K^*}$ ,  $F_\rho$ . The values for  $B(B^- \rightarrow K^{*-}\gamma)$  are very close to those for  $B(\bar{B} \rightarrow \bar{K}^{*0}\gamma)$  with the main shift coming from the different lifetimes. For central input parameters we find  $B(B^- \rightarrow K^{*-}\gamma) = 7.45 \cdot 10^{-5}$  compared to  $B(\bar{B} \rightarrow \bar{K}^{*0}\gamma) = 7.09 \cdot 10^{-5}$ . The CP asymmetry  $\mathcal{A}_{CP}(K^*\gamma)$  is typically  $-0.5\%$ .

Taking the sizable uncertainties into account, the results for  $B \rightarrow K^*\gamma$  in Table 2 are compatible with the experimental measurements in (2) and (3), even though the central theoretical values appear to be somewhat high.

The direct CP asymmetry, which is substantial for the  $\rho\gamma$  modes, is much less dependent on the form factors. Here the largest theoretical uncertainty comes from the scale dependence. This is to be expected because the direct CP asymmetry is proportional to the perturbative strong phase difference, which arises at  $\mathcal{O}(\alpha_s)$ . Unknown power corrections could have some impact on the predic-

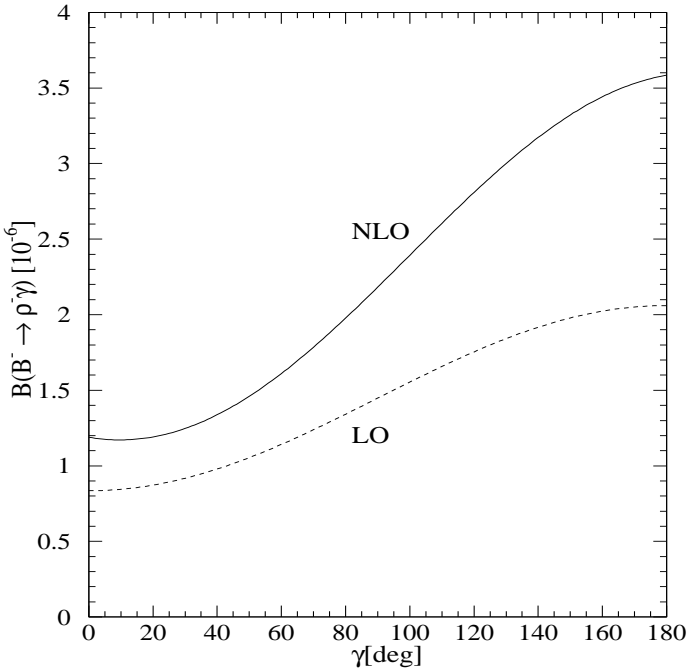


Figure 9: The branching fraction  $B(B^- \rightarrow \rho^- \gamma)$  as a function of the CKM angle  $\gamma$  at leading and next-to-leading order.

tion.  $B \rightarrow \rho\gamma$  also depends sensitively on fundamental CKM parameters, such as  $|V_{ub}/V_{cb}|$  and  $\gamma$ , and can thus in principle serve to constrain the latter quantities once measurements become available. This is further illustrated in Figs. 9 and 10, where the dependence on  $\gamma$  is shown for  $B(B^- \rightarrow \rho^- \gamma)$  and  $\mathcal{A}_{CP}(\rho\gamma)$ , respectively.

Further interesting observables are the isospin breaking quantities

$$\Delta_{+0} = \frac{\Gamma(B^+ \rightarrow \rho^+ \gamma)}{2\Gamma(B^0 \rightarrow \rho^0 \gamma)} - 1 \quad (56)$$

$$\Delta_{-0} = \frac{\Gamma(B^- \rightarrow \rho^- \gamma)}{2\Gamma(\bar{B}^0 \rightarrow \rho^0 \gamma)} - 1 \quad (57)$$

$$\Delta(\rho\gamma) = \frac{\Delta_{+0} + \Delta_{-0}}{2} \quad (58)$$

Within our approximations, isospin breaking is generated by weak annihilation. Isospin breaking was already discussed in [26], partially including NLO corrections. Our results, including the power-suppressed annihilation effects at leading order in QCD, together with the complete NLO expressions at leading power, are displayed in Fig. 11. We remark that our sign of  $\Delta(\rho\gamma)$  differs from the one found in [26].

Another application of our results concerns an estimate of U-spin breaking effects in  $B \rightarrow V\gamma$  decays. U-spin symmetry, the symmetry of strong interactions

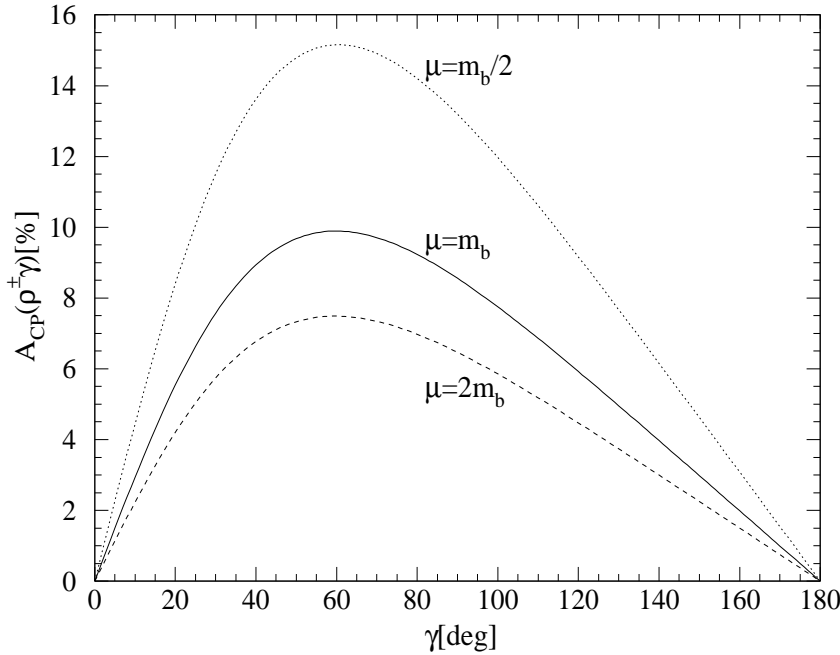


Figure 10: The CP asymmetry  $A_{CP}(\rho\gamma)$  as a function of the CKM angle  $\gamma$  for three values of the renormalization scale  $\mu = m_b/2$ ,  $m_b$  and  $2m_b$ .

under exchange of  $d$  and  $s$  quarks, has been advocated as a tool to control hadronic uncertainties in tests of the Standard Model [27, 28, 29]. Defining

$$\Delta B(B \rightarrow K^*\gamma) = B(B^+ \rightarrow K^{*+}\gamma) - B(B^- \rightarrow K^{*-}\gamma) \quad (59)$$

$$\Delta B(B \rightarrow \rho\gamma) = B(B^+ \rightarrow \rho^+\gamma) - B(B^- \rightarrow \rho^-\gamma) \quad (60)$$

the quantity

$$\Delta B(B \rightarrow K^*\gamma) + \Delta B(B \rightarrow \rho\gamma) \equiv 0 \quad (61)$$

in the limit of U-spin symmetry and within the Standard Model. This has been discussed in [27] and was considered in more detail in [28]. Using our expressions and central values for all parameters we find

$$\Delta B(B \rightarrow K^*\gamma) = -7 \cdot 10^{-7} \quad (62)$$

$$\Delta B(B \rightarrow \rho\gamma) = 4 \cdot 10^{-7} \quad (63)$$

where we have chosen the CKM angle  $\gamma = \pi/2$ , which maximises the effects. The two quantities indeed have opposite signs, but their sum only partly cancels, leaving a U-spin breaking remainder of  $-3 \cdot 10^{-7}$ . This effect is almost entirely due to the difference  $(F_{K^*} - F_\rho)$ . For form-factor values different from those in Table 1, the U-spin breaking effect would approximately be rescaled proportional to  $(F_{K^*} - F_\rho)$ . For our choice the sum of the two asymmetries in (61) is of the

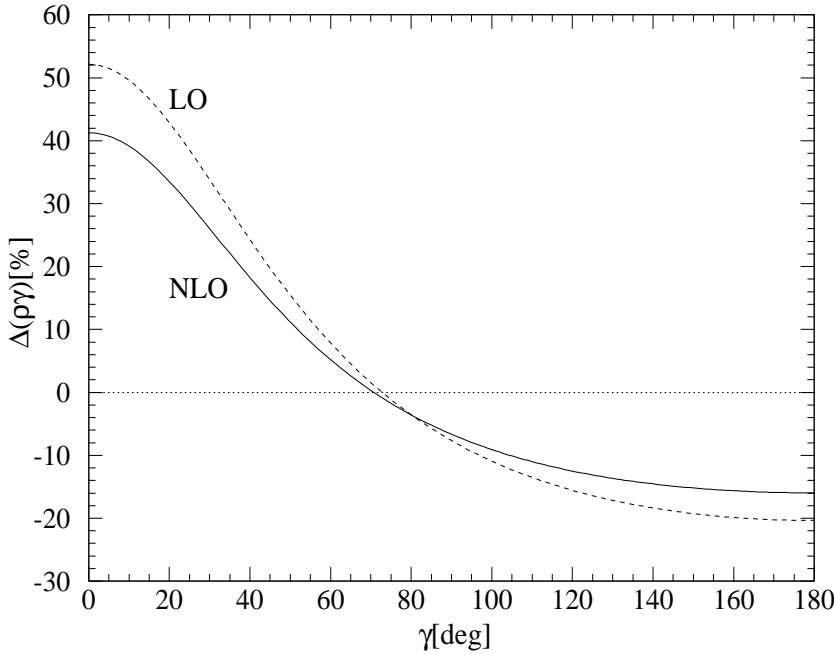


Figure 11: The isospin-breaking asymmetry  $\Delta(\rho\gamma)$  as a function of the CKM angle  $\gamma$  at leading and next-to-leading order.

same order of magnitude as the individual asymmetries. This example quantifies the limitations of the relation (61) as a Standard Model test.

## 6 Conclusions

In this paper we have discussed a systematic and model-independent framework for the exclusive radiative decays  $B \rightarrow V\gamma$  based on the heavy-quark limit. This allowed us to compute the decay amplitudes for these modes consistently at next-to-leading order in QCD.

An important conceptual aspect of this analysis is the interpretation of loop contributions with charm and up quarks, which come from leading operators in the effective weak Hamiltonian. We have argued that these effects are calculable in terms of perturbative hard-scattering functions and universal meson light-cone distribution amplitudes. They are  $\mathcal{O}(\alpha_s)$  corrections, but are leading power contributions in the framework of QCD factorization. This picture is in contrast to the common notion that considers charm and up-quark loop effects as generic, uncalculable long-distance contributions. Non-factorizable long-distance corrections may still exist, but they are power-suppressed.

Another important feature of the NLO calculation are the strong interaction phases, which are calculable at leading power. They play a crucial role for CP

violating observables.

We have seen that weak-annihilation amplitudes are power-suppressed, but can be numerically important for  $B \rightarrow \rho\gamma$  because they enter with large coefficients. These effects also turn out to be calculable and were included in our phenomenological discussion at leading order in QCD.

Finally, we have presented a numerical analysis of important observables, including the branching ratios of  $B \rightarrow K^*\gamma$ ,  $B \rightarrow \rho\gamma$ , and CP asymmetries and isospin-breaking in  $B \rightarrow \rho\gamma$  decays (see sec. 5). Currently, the large uncertainties in the  $B \rightarrow V$  form factors are still an important limitation, but the situation can be systematically improved. In particular, our approach allows for a consistent perturbative matching of the nonperturbative form factor to the short-distance part of the amplitude. Our formalism can also be applied to other radiative rare  $B$  decays, such as  $B_s \rightarrow V\gamma$ ,  $V = \phi, K^*$ , or  $B_d \rightarrow \omega\gamma$  (see e.g. [25] for a discussion of these modes).

The improved theoretical understanding of  $B \rightarrow V\gamma$  decay observables strengthens the motivation for still more detailed experimental investigations, which will contribute significantly to our knowledge of the flavour sector.

## Acknowledgements

While this paper was being written, we became aware of the work in ref. [30] where a similar subject is treated. We thank Martin Beneke for useful discussions and communications on the results of [30] prior to publication. Thanks are also due to Josip Trampetić for discussions. S.W.B. gratefully acknowledges financial support from the Studienstiftung des deutschen Volkes and thanks the CERN Theory Division for the kind hospitality.

## Note Added

After completion of this work we received the manuscript [31] discussing  $B \rightarrow \rho\gamma$  decays at next-to-leading order in QCD. The calculation uses the framework of [15, 16] and of [20], and is similar in spirit to the analysis presented here. We disagree, however, with several of the main results given in [31]. First, the expressions corresponding to our functions  $H_1(0)$  and  $H_8$  are missing a factor of  $-4$  and  $-1$ , respectively, in [31]. Furthermore, the charm contribution  $H_1(s_c)$  is approximated by  $H_1(0)$ . As can be seen from our results, this approximation is not suitable. It gives a real part with the wrong sign and misses a complex phase, which is important for  $\mathcal{A}_{CP}(\rho\gamma)$  (changing the asymmetry in Table 2 from 9.9% to 13.2%). Finally, we find  $H_1(s_c)$  to be free of infrared divergences, also for non-vanishing charm-quark mass, contrary to [31]. This is important conceptually, because such a divergence could not be reabsorbed into the form factor and would signify a breakdown of the factorization approach.

## References

- [1] F. Blanc [CLEO Collaboration], talk presented at the XXXVIth Rencontres de Moriond, Electroweak Interactions and Unified Theories, Les Arcs, France, March 2001.
- [2] G. Taylor, [BELLE Collaboration], talk presented at the XXXVIth Rencontres de Moriond, Electroweak Interactions and Unified Theories, Les Arcs, France, March 2001.
- [3] R. Barate *et al.* [ALEPH Collaboration], Phys. Lett. B **429** (1998) 169.
- [4] T. E. Coan *et al.* [CLEO Collaboration], Phys. Rev. Lett. **84** (2000) 5283.
- [5] T. Pulliam [BABAR Collaboration], talk presented at PHENO 2001, Madison, Wisconsin, May 2001, BaBar-Talk-01/53.
- [6] S. Bertolini, F. Borzumati and A. Masiero, Phys. Rev. Lett. **59** (1987) 180.
- [7] A. Ali, C. Greub and T. Mannel, DESY-93-016, *To be publ. in Proc. of ECFA Workshop on the Physics of a B Meson Factory, Eds. R. Aleksan, A. Ali, 1993.*
- [8] A. J. Buras, M. Misiak, M. Münz and S. Pokorski, Nucl. Phys. B **424** (1994) 374.
- [9] M. Ciuchini *et al.*, Phys. Lett. B **316** (1993) 127; M. Ciuchini, E. Franco, L. Reina and L. Silvestrini, Nucl. Phys. B **421** (1994) 41.
- [10] K. Adel and Y. Yao, Phys. Rev. D **49** (1994) 4945; C. Greub and T. Hurth, Phys. Rev. D **56** (1997) 2934; A. J. Buras, A. Kwiatkowski and N. Pott, Nucl. Phys. B **517** (1998) 353.
- [11] C. Greub, T. Hurth and D. Wyler, Phys. Rev. D **54** (1996) 3350; A. J. Buras, A. Czarnecki, M. Misiak and J. Urban, hep-ph/0105160.
- [12] K. Chetyrkin, M. Misiak and M. Münz, Phys. Lett. B **400** (1997) 206; Erratum-ibid. B **425** (1998) 414.
- [13] M. Misiak, hep-ph/0002007; C. Greub, hep-ph/9911348.
- [14] H. H. Asatrian, H. M. Asatrian and D. Wyler, Phys. Lett. B **470** (1999) 223; C. Greub, H. Simma and D. Wyler, Nucl. Phys. B **434** (1995) 39 [Erratum-ibid. B **444** (1995) 447]
- [15] M. Beneke, G. Buchalla, M. Neubert and C. T. Sachrajda, Phys. Rev. Lett. **83** (1999) 1914.
- [16] M. Beneke, G. Buchalla, M. Neubert and C. T. Sachrajda, Nucl. Phys. B **591** (2000) 313.

- [17] P. Ball and V. M. Braun, Phys. Rev. D **58** (1998) 094016.
- [18] J. M. Flynn and C. T. Sachrajda, hep-lat/9710057.
- [19] J. Charles *et al.*, Phys. Rev. D **60** (1999) 014001.
- [20] M. Beneke and T. Feldmann, Nucl. Phys. B **592** (2001) 3.
- [21] G. Burdman and G. Hiller, hep-ph/0011266.
- [22] G. Buchalla, A. J. Buras and M. E. Lautenbacher, Rev. Mod. Phys. **68** (1996) 1125.
- [23] A. Ali, V. M. Braun and H. Simma, Z. Phys. C **63** (1994) 437.
- [24] P. Ball and V. M. Braun, Phys. Rev. D **54** (1996) 2182.
- [25] B. Grinstein and D. Pirjol, Phys. Rev. D **62** (2000) 093002.
- [26] A. Ali, L. T. Handoko and D. London, hep-ph/0006175.
- [27] M. Gronau and J. L. Rosner, Phys. Lett. B **500** (2001) 247; M. Gronau, Phys. Lett. B **492** (2000) 297.
- [28] T. Hurth and T. Mannel, hep-ph/0103331.
- [29] R. Fleischer, Phys. Lett. B **459** (1999) 306.
- [30] M. Beneke, T. Feldmann and D. Seidel, RWTH Aachen preprint PITHA 01/05, hep-ph/0106067.
- [31] A. Ali and A. Y. Parkhomenko, hep-ph/0105302.